IAI Journals.ASM.org

# The Assembly of GM1 Glycolipid- and Cholesterol-Enriched Raft-Like Membrane Microdomains Is Important for Giardial Encystation

**Atasi De Chatterjee,[a,c] Tavis L. Mendez,[a,c] Sukla Roychowdhury,[b,c] Siddhartha Das[a,c]**

Infectious Disease and Immunology[a] and Neuromodulation Disorders Clusters,[b] Border Biomedical Research Center, and Department of Biological Sciences,[c] University of Texas at El Paso, El Paso, Texas, USA

**Although encystation (or cyst formation) is an important step of the life cycle of *Giardia*, the cellular events that trigger encystation are poorly understood. Because membrane microdomains are involved in inducing growth and differentiation in many eukaryotes, we wondered if these raft-like domains are assembled by this parasite and participate in the encystation process. Since the GM1 ganglioside is a major constituent of mammalian lipid rafts (LRs) and known to react with cholera toxin B (CTXB), we used Alexa Fluor-conjugated CTXB and GM1 antibodies to detect giardial LRs. Raft-like structures in trophozoites are located in the plasma membranes and on the periphery of ventral discs. In cysts, however, they are localized in the membranes beneath the cyst wall. Nystatin and filipin III, two cholesterol-binding agents, and oseltamivir (Tamiflu), a viral neuraminidase inhibitor, disassembled the microdomains, as evidenced by reduced staining of trophozoites with CTXB and GM1 antibodies. GM1- and cholesterol-enriched LRs were isolated from *Giardia* by density gradient centrifugation and found to be sensitive to nystatin and oseltamivir. The involvement of LRs in encystation could be supported by the observation that raft inhibitors interrupted the biogenesis of encystation-specific vesicles and cyst production. Furthermore, culturing of trophozoites in dialyzed medium containing fetal bovine serum (which is low in cholesterol) reduced raft assembly and encystation, which could be rescued by adding cholesterol from the outside. Our results suggest that *Giardia* is able to form GM1- and cholesterol-enriched lipid rafts and these raft domains are important for encystation.**

*Giardia lamblia*, an intestinal protozoan, is responsible for a waterborne infection (known as giardiasis) worldwide (1). Giardiasis can be symptomatic or asymptomatic. In its acute stage, giardiasis can lead to steatorrhea, sporadic or recurrent diarrhea, and weight loss. Chronic infection can lead to diseases such as gallbladder ulcer or peptic ulcer (2). Giardiasis, which can also be caused by zoonotic infection, is transmitted via infective cysts through contaminated food and water (1). Exposure of cysts to gastric acid during passage through the human stomach triggers excystation, while factors in the small intestine, where trophozoites colonize, induce encystation or cyst formation (3). During colonization in the small intestine of humans, trophozoites are exposed to various dietary proteins, fatty acids, and lipids. It has previously been reported that factors located in the duodenum and jejunum (where trophozoites preferably colonize) play important roles in supporting the growth and encystation of *Giardia* (4). Dietary fatty acids or fatty acids generated from intestinal lipids by the action of lipases have been shown to be toxic to *Giardia* trophozoites. Studies indicate that while free fatty acids kill *Giardia* trophozoites, bile salts protect them from fatty acid-induced cell death (5–7). Thus, proper concentrations of bile acids, fatty acids, and other intestinal factors are important for the survival, growth, and encystation of *Giardia* in the small intestine of humans.

*Giardia* has a limited lipid and fatty acid synthesis ability (8). Therefore, it appears that the majority of lipids are obtained by this parasite from a growth medium or from the small intestinal milieu (9). Some of the acquired lipids undergo remodeling by the head group and fatty acid exchange reactions. Fatty acids can undergo chain shortening or elongation before incorporation into the plasma membranes (10–12). Most recently, we have demonstrated that glucosylceramide transferase (GlcT1), an enzyme of the sphingolipid pathways, serves as a key regulator of encystation and viable cyst production by *Giardia* (13). However, it is not known how the process of encystation is initiated and if the plasma membranes of trophozoites participate in this process. Because membrane rafts are present in the majority of eukaryotic cells and involved in cellular differentiation, we postulate that *Giardia* assembles raft-like microdomains and the molecules that are associated with giardial rafts take part in the encystation process.

In this paper, we show for the first time that *Giardia* has the ability to assemble cholesterol- and GM1 ganglioside-enriched membrane microdomains. Disassembly of these microdomains affects encystation and cyst production. Depletion of cholesterol from the culture medium also interferes with raft assembly and cyst formation and produces atypical (non-type I) cysts that express both trophozoite and cyst proteins instead of mostly cyst proteins. The addition of cholesterol rescues this process by assembling raft-like microdomains and generating cysts with classical oval morphologies.

**Received** 22 December 2014 **Returned for modification** 15 January 2015
**Accepted** 22 February 2015

**Accepted manuscript posted online** 2 March 2015

**Citation** De Chatterjee A, Mendez TL, Roychowdhury S, Das S. 2015. The assembly of GM1 glycolipid- and cholesterol-enriched raft-like membrane microdomains is important for giardial encystation. Infect Immun 83:2030–2042. doi:10.1128/IAI.03118-14.

**Editor:** J. H. Adams

Address correspondence to Siddhartha Das, sdas@utep.edu.

Supplemental material for this article may be found at http://dx.doi.org/10.1128/IAI.03118-14.



doi:10.1128/IAI.03118-14

## MATERIALS AND METHODS

**Materials.** Lipid raft (LR) inhibitors (i.e., nystatin and filipin III) were purchased from Sigma-Aldrich Co., LLC (St. Louis, MO). Oseltamivir (Tamiflu; a viral neuraminidase inhibitor) and myriocin (an inhibitor of sphingolipid synthesis) were purchased from Selleckchem (Houston, TX) and Sigma-Aldrich, respectively. Stock solutions of nystatin (25 mM), filipin III (25 mM), and oseltamivir (12.18 mM) were prepared in dimethyl sulfoxide (DMSO; Sigma-Aldrich). Myriocin (12.45 mM) was dissolved in methanol (Sigma-Aldrich). All other reagents were of analytical grade and obtained in the highest-purity grades from Sigma-Aldrich. Adult bovine serum (ABS; catalogue no. SH30075.03) and dialyzed fetal bovine serum (DFBS; catalogue no. 26400-044) were purchased from HyClone (UT, USA) and Gibco Invitrogen Inc. (Carlsbad, CA), respectively. A fluorescent LR labeling kit (Vybrant Alexa Fluor 488) and 1,1′-dilinoleyl-3,3,3′,3′-tetramethylindocarbocyanine perchlorate [Dil$\Delta^{9,12}$-$C_{18}$(3), $ClO_4$; FAST Dil oil] were purchased from Gibco Invitrogen (Carlsbad, CA). Fluorescein isothiocyanate (FITC)-conjugated trophozoite antibody (antirat polyclonal antibody; catalogue no. A900; Troph-O-Glo; Waterborne Inc., New Orleans, LA), Alexa Fluor 568-conjugated donkey antimouse antibody, and anti-ganglioside GM1 rabbit polyclonal antibody were purchased from Waterborne Inc. (New Orleans, LA), Gibco Invitrogen (Carlsbad, CA), and Abcam (Cambridge, MA), respectively. Mouse monoclonal cyst antibody and FITC-conjugated goat antirabbit secondary antibody were purchased from Santa Cruz Biotechnology, Inc. (Santa Cruz, CA).

**Cell culture.** *G. lamblia* trophozoites (ATCC 30957, strain WB), clone C6, were cultivated in TYI-S-33 medium supplemented with 5% ABS or DFBS and 0.5 mg/ml adult bovine bile (14, 15). The antibiotic piperacillin (100 μg/ml) was added during routine culture of *Giardia* (16). Parasites were detached by chilling on ice, harvested by centrifugation at 1,500 × *g* for 10 min at 4°C, repeatedly washed in phosphate-buffered saline (PBS), and counted with the help of a hemocytometer under a light microscope (phase-contrast). *In vitro* encystation was carried out by culturing trophozoites in TYI-S-33 medium supplemented with 5% ABS (which is cholesterol enriched) or DFBS (which has a low level of cholesterol) and bovine bile (i.e., 5 mg/ml; high-bile medium) at pH 7.8 as described previously by Kane et al. (17).

**Treatment with inhibitors.** To examine the effects of inhibitors on growth and encystation, trophozoites were inoculated (~1 × $10^6$ cells/ml) in 4-ml glass vials containing TYI-S-33 medium (1 ml, no serum, pH 7.1) and treated with various concentrations (0, 5, 10, 20, and 50 μM) of inhibitors (nystatin, filipin III, and oseltamivir) for 30 min at 37°C. After treatment, the vials were filled with TYI-S-33 medium (pH 7.1) supplemented with bovine bile (0.5 mg/ml) and ABS (5%) or DFBS (5%) and incubated for 24 h at 37°C. After separating the attached viable cells from the nonattached cells by decanting the medium, they were washed with PBS, resuspended in cold PBS, kept on ice for 30 min, and counted under a microscope using a hemocytometer. To examine the effects on cyst formation, encystation was carried out in the presence of inhibitors for the specific times described below. Encysting trophozoites and *in vitro*-derived cysts were collected by centrifugation (1,500 × *g* for 5 min) and processed accordingly. Water-resistant cysts were obtained by treating the cells in cold distilled water (4°C) overnight, isolated by centrifugation, and counted. For confocal microscopy, trophozoites and encysting cells were fixed in 4% paraformaldehyde, mounted with ProLong Gold antifade reagent (Invitrogen), mixed with DAPI (4′,6-diamidino-2-phenylindole), and observed under an LSM 700 confocal microscope (Zeiss Carl Zeiss Laser Scanning Systems).

**Identification of lipid rafts in *Giardia*.** Control and inhibitor-treated *Giardia* trophozoites, encysting cells, and cysts were isolated by centrifugation (1,500 × *g* for 5 min), washed in PBS, and stained with cholera toxin B (CTXB) or GM1 antibody. For CTXB labeling, ~1 × $10^7$ cells were taken, washed in PBS, and reacted with CTXB conjugated to Alexa Fluor 488 (1 μg/ml) for 10 min, followed by labeling with CTXB antibody (1:200 dilution) for 15 min, as recommended by the Vybrant lipid raft labeling kit manufacturer (Invitrogen). The cells were then fixed with 4% paraformaldehyde.

For immunostaining with GM1 antibody, cells (~1 × $10^7$) were fixed with 4% paraformaldehyde in PBS and blocked in 5% normal goat serum for 1 h. Slides were washed three times and incubated with GM1-specific polyclonal antisera (1:50 dilution; Abcam, Cambridge, MA) overnight at 4°C, followed by exposure to a secondary antibody (goat anti-rabbit IgG) conjugated to Alexa Fluor 568 (1:500 dilution) for 1 h. Both CTXB- and GM1-labeled cells were mounted with ProLong Gold antifade reagent with DAPI (Invitrogen) and visualized by confocal microscopy (LSM 700 confocal microscope; Carl Zeiss Laser Scanning Systems). For the identification of nonraft lipids, trophozoites were incubated with FAST Dil oil (1 μM) for 2 min at room temperature, fixed with paraformaldehyde (4%), and examined under a confocal microscopy as previously described (13, 18).

**Measurement of cholesterol levels in trophozoites and serum using a cholesterol assay kit.** Trophozoites were cultured in Diamond's TYI-S-33 medium containing serum (5% ABS or DFBS) and bovine bile (0.5 mg/ml), as mentioned above. Cells were harvested and lysed, and the cholesterol concentration was measured using an Amplex red cholesterol assay kit (Invitrogen) with a fluorescence microplate reader (absorption, 530 nm; emission, 590 nm). Serum (ABS and DFBS) cholesterol contents were also measured side-by-side with trophozoite cholesterol contents.

**Labeling of *Giardia* with trophozoite and cyst antibodies.** To monitor the expression of trophozoite proteins, nonencysting and encysting trophozoites and water-resistant cysts were fixed in 4% paraformaldehyde for 15 min and labeled with FITC-conjugated trophozoite antibody (antirat polyclonal antibody; Troph-O-Glo; Waterborne Inc., New Orleans, LA) following the instructions provided by the manufacturer. Troph-O-Glo is a trophozoite antibody that recognizes trophozoites only and not cysts (see Fig. 3B). For cyst proteins, cyst antibody (1:100, monoclonal; Santa Cruz Biotechnology, Inc., Santa Cruz, CA) was employed and Alexa Fluor 568 donkey anti-mouse IgG (Invitrogen) was used as a secondary antibody (1:500 dilution); the cells were incubated for 1 h, mounted with ProLong Gold antifade reagent with DAPI (Invitrogen), and visualized by confocal microscopy (LSM 700 confocal microscope; Carl Zeiss Laser Scanning Systems). Previously, we have shown that this cyst antibody recognizes the cyst wall proteins 1, 2, and 3 and does not cross-react with trophozoites (13). The fluorescence intensities were quantified with the help of Zeiss Zen 2009 confocal software (Carl Zeiss).

**Cholesterol supplementation.** *Giardia* trophozoites were cultured in TYI-S-33 medium (14, 15) containing DFBS. For encystation, attached trophozoites were separated from nonattached cells by decanting the medium, and the culture was then replenished with fresh encystation medium as described previously (16). For cholesterol supplementation experiments, different concentrations of cholesterol (100, 215, and 300 μg/ml) were added to DFBS-containing encystation medium and the mixture was incubated for 18 h. We used 215 μg/ml (21.5%) of cholesterol in all of our experiments, as 100 μg/ml was unable to produce any remarkable effect and at a concentration of 300 μg/ml cholesterol precipitated out of the solution. In some experiments, nystatin (27 μM) and filipin III (7.6 μM) were added in cholesterol-supplemented medium to determine if additional cholesterol can reverse the effects of these two cholesterol-binding agents, as described below.

**Isolation of giardial lipid rafts.** Lipid rafts were isolated by OptiPrep density gradient centrifugation following the protocol described in the Sigma-Aldrich Catalogue (catalogue no. CS 0750; caveolae/rafts isolation kit). Approximately $10^9$ attached trophozoites were harvested as described above, resuspended in CTXB-horseradish peroxidase (HRP) solution (1:500 in PBS; Sigma-Aldrich, St. Louis, MO), and kept on ice for 1 h (19, 20). The cells were washed several times in PBS, mixed with lysis buffer (5 mM Tris-HCl, pH 7.8, 2 mM EDTA, 0.4 mM dithiothreitol) containing 1% Triton X-100 and a protease inhibitor cocktail, and incubated on ice for 30 min. The cell lysate was mixed with 35% OptiPrep density gradient medium (Sigma-Aldrich, St. Louis, MO), followed by step overlays with 30%, 25%, 20%, and 0% OptiPrep, and centrifuged at

200,000 × *g* for 4 h with a Sorvall T-865.1 fixed-angle rotor (Sorvall WX Ultra series centrifuge; Thermo Scientific, IL). Fractions of 1 ml were collected from the top of the gradient and analyzed by enzyme-linked immunosorbent assay (ELISA) as described below.

**ELISA.** An ELISA was performed to assess CTXB-HRP-enriched LR fractionation following the method of Blank et al. (20), with some modifications. The fractions were collected and mixed with carbonate-bicarbonate buffer (pH 9.6) containing bovine serum albumin (1%), followed by blocking for 1 h at 37°C, and then washed with PBS containing 0.05% Tween 20 (PBST), before they were reacted with chemiluminescent reagent (Thermo Scientific, IL) following the instructions provided by the manufacturer. The cholesterol contents in the gradient fractions were measured using the Amplex red cholesterol assay kit (Invitrogen).

**Statistical analysis.** For intensity measurements, cells were randomly selected from 10 to 15 fields from 3 to 5 separate experiments. Unless otherwise specified, approximately 50 cells were considered for each condition and were analyzed by Zeiss 2009 Zen confocal software. For counting of cells (trophozoites or cysts), a total of 75 to 200 cells from 6 to 15 randomly selected microscopic fields from 2 to 3 experiments were counted, and data are expressed as the mean ± standard deviation (SD). One-way analyses of variance (ANOVAs) followed by the Holm-Šídák or Tukey method were performed using Sigma Plot (version 12) software to evaluate differences between the treatment and the control groups. Student's *t* tests were performed for the results shown in Fig. 5A and B, and a *P* value of $<0.05$ was considered statistically significant.

## RESULTS

***Giardia* assembles raft-like microdomains.** Membrane microdomains or LRs were found in the majority of eukaryotic cells. The LRs are involved in various cellular functions, including cell differentiation, cell adhesion, and membrane signaling (19, 20); therefore, it is conceivable that they are also present in *Giardia* and participate in cellular differentiation and other cellular functions. To identify the raft-like microdomains, trophozoites were labeled with commercially available fluorescently conjugated cholera toxin B (CTXB). CTXB is known to bind with the GM1 ganglioside of the membrane microdomains (20). We observed that CTXB reactions were mostly localized in the plasma membranes, on the periphery of the ventral disc, and in the flagella of trophozoites (Fig. 1A, image a). A similar type of CTXB labeling of *Giardia* trophozoites was also reported earlier by Stefanić et al. (21). Side-by-side with CTXB, parasites were labeled with GM1 antibody to stain raft-like structures. Nguyen and Hildreth (22) previously used GM1 antibody to label the LRs of HIV-1-infected Jurkat cells. It was noted that immunostaining with GM1 antibody revealed discrete and dotted raft-like structures located in the plasma membranes and in the caudal flagella (Fig. 1A, image b). These typical raft structures were also visible in a three-dimensional (3D) image of a *Giardia* trophozoite after labeling with CTXB (Fig. 1B). To distinguish raft lipids from non-raft lipids, a lipophilic dialkylcarbocyanine tracer (or FAST Dil oil) was used (13, 18). Unlike CTXB and GM1 antibody, FAST Dil oil stained the cytoplasmic and endoplasmic reticulum/perinuclear membrane lipids (non-raft lipids) with a very different staining pattern (Fig. 1A, image c).

Because cholesterol is a major component of raft-like microdomains (23, 24), we tested the effects of two cholesterol-binding agents (i.e., nystatin [27 μM] and filipin III [7.6 μM]) on raft assembly by *Giardia* cultured in ABS-supplemented medium. It was observed that both inhibitors lowered the CTXB reactivity of trophozoites (Fig. 2A, images b and c). Also, oseltamivir, a viral neuraminidase (sialidase) inhibitor, reduced the staining of trophozoites by CTXB and GM1 antibody (Fig. 2A, image d). Because giardial rafts contain GM1 ganglioside (Fig. 1) and oseltamivir affects the neuronal GM1 level (25), we thought that the alteration of GM1 levels in *Giardia* should also interfere with the assembly of raft-like microdomains. Figure 2A (image d) demonstrates that CTXB reactivity in trophozoites was low after oseltamivir (20 μM) treatment. Like CTXB, immunostaining with GM1 antibody was also affected by these three inhibitors (Fig. 2A, images b′ to d′). Although all of these inhibitors were effective in reducing the intensity of GM1 labeling (Fig. 2A, images a′ to d′), maximum inhibition by oseltamivir was observed. Myriocin, an inhibitor of 3-keto-sphinganine synthesis (26), which we used for comparison, did not significantly influence CTXB and GM1 antibody labeling (Fig. 2B and C, images e and e′). Quantitative assessments of the actions of the inhibitors on CTXB and GM1 antibody labeling of trophozoites are shown in Fig. 2B and C.

The doses that we used in the current study were determined from dose-response curves, and their respective 50% inhibitory concentrations ($IC_{50}$s) are shown in Table 1. It is clear that the $IC_{50}$s for nystatin, filipin III, and oseltamivir ranged from 36 to 49 μM. Depending on the conditions and cell types in some cases,

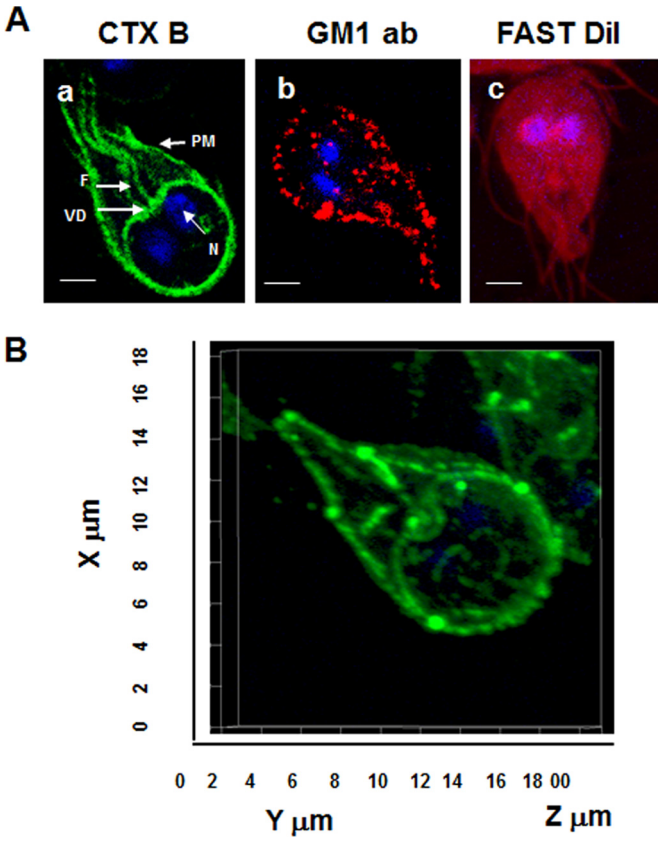


**FIG 1** Raft-like microdomains in *Giardia* trophozoites. Trophozoites were labeled with Alexa Fluor 488-conjugated CTXB (image a, green) and GM1 antibody (image b, red). Labeling of plasma membranes, the ventral disc, and the flagella of trophozoites is visible. FAST Dil oil labels the cytoplasmic and nuclear lipids of trophozoites (image c). DAPI-stained nuclei are also noticeable. N, nucleus; PM, plasma membrane; F, flagella; VD, ventral disc; ab, antibody. Bars, 5 μm. (B) 3D representation. The image of CTXB-labeled *Giardia* trophozoites was captured using Zen 2009 software. z-stacks were acquired, and a 3D model was reconstructed from the 12 optical sections of the z-stacks with a slice thickness of 0.37 μm each.

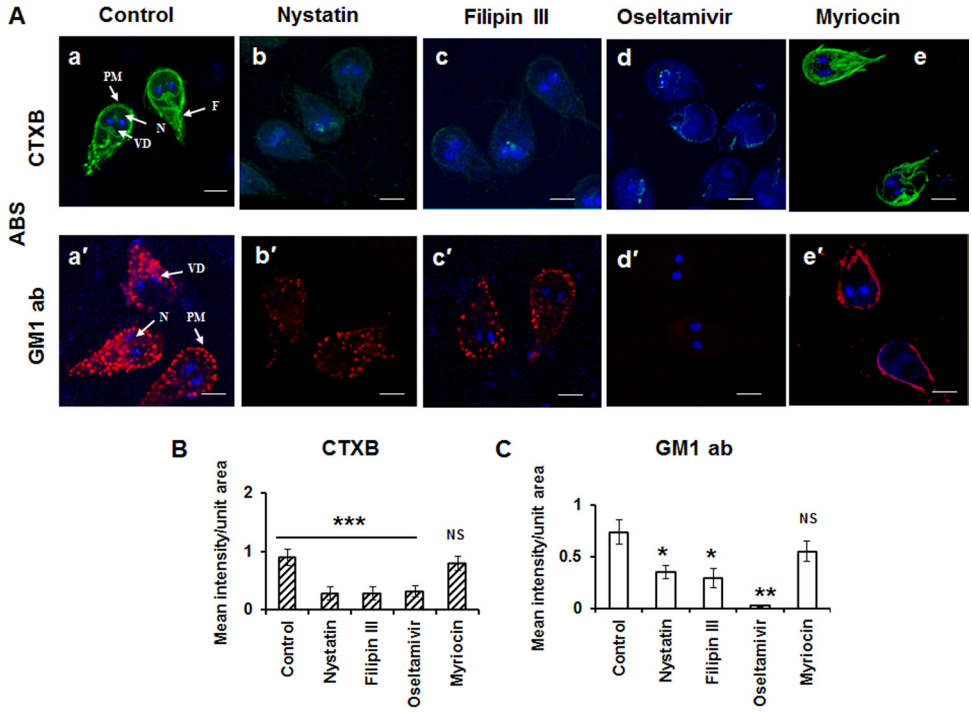


**FIG 2** Nystatin, filipin III, and oseltamivir inhibit the labeling of trophozoites by CTXB and GM1 antibodies. (A) Trophozoites were treated with nystatin (27 μM), filipin III (7.6 μM), and oseltamivir (20 μM) for 30 min before labeling with Alexa Fluor-conjugated CTXB antibody (images a to d) and GM1 antibody (images a′ to d′). Myriocin (27 μM), a sphingolipid inhibitor, was used as a negative control (images e and e′). N, nucleus; PM, plasma membrane; F, flagella; VD, ventral disc. Bars, 5 μm. (B and C) Changes in intensity of control and inhibitor-treated trophozoites. For intensity measurements, cells were randomly selected from 10 to 15 fields from 3 to 5 separate experiments. Approximately 50 cells were considered for each condition and were analyzed using Zeiss Zen 2009 confocal software. One-way ANOVAs were performed to evaluate differences (means ± SDs) between the treatment and control groups. Mean intensities from 3 to 5 separate experiments are shown in panels B and C. Statistical significance was calculated using a one-way ANOVA test, followed by the Tukey (B) and Holm-Šídák (C) methods. *, $P < 0.05$; **, $P < 0.01$; ***, $P < 0.001$; NS, not significant.

their concentrations did not even reach their $IC_{50}$s. Figure S1 in the supplemental material represents the effects of these inhibitors on CTXB labeling of *Giardia* trophozoites. As evidenced from Fig. S1, all of these inhibitors were effective in reducing CTXB labeling in a dose-dependent manner, and maximum levels of inhibition were observed at 50 μM concentrations. However, we used concentrations much lower than 50 μM to avoid off-target effects and toxicity. For example, the concentrations of nystatin and filipin III used in the current study were 27 μM and 7.6 μM, respectively. Puri et al. (23) and Pohl et al. (24) previously used the same concentrations of these two inhibitors in blocking the raft-mediated endocytosis by skin fibroblasts and HepG2 cells, respectively. The concentration of oseltamivir (20 μM) that was chosen was lower than 50 μM (Table 1; see also Fig. S1 in the supplemental material). At this concentration of oseltamivir (20 μM), we observed that more than 90% of the cells remained viable (not shown); only the attached cells were considered viable and counted. As opposed to the doses used in the current study, in an earlier study, 10 mM methyl-β-cyclodextrin (MBCD; an inhibitor of lipid rafts) was used to evaluate the role of membrane microdomains on the adhesion of trophozoites on cultured enterocyte-like Caco-2/TC-7 cells (27).

**TABLE 1** $IC_{50}$s of nystatin, filipin III, and oseltamivir for trophozoites and cysts[a]

| *Giardia* | Mean ± SD $IC_{50}$ (μM) | | |
|---|---|---|---|
| | Nystatin | Filipin III | Oseltamivir |
| Trophozoites cultured in ABS medium | — | 42 ± 0.02 | — |
| Cysts encysted in ABS medium | 40 ± 0.05 | 43 ± 0.04 | 49 ± 0.007 |
| Trophozoites cultured in DFBS medium | — | — | — |
| Cysts encysted in DFBS medium | 37 ± 0.09 | 46 ± 0.06 | — |

[a] $IC_{50}$, concentrations that caused 50% growth inhibition of trophozoites and 50% inhibition of cyst formation; —, the concentration did not reach the $IC_{50}$; ABS, adult bovine serum; DFBS, dialyzed fetal bovine serum.

**The assembly of giardial microdomains is important for encystation.** It has previously been postulated that cyst morphologies are indicative of cyst viability/infectivity and cysts with classical type I morphologies are competent to undergo excystation *in vitro* (16). However, it is unclear how trophozoites are transformed into cysts. Since raft-like membrane microdomains are involved in regulating the growth and differentiation of bacteria and higher eukaryotes (28, 29), we thought that raft microdomains in *Giardia* also participate in encystation and cyst production. We also questioned if the immunostaining pattern of giardial rafts changes during the process of stage differentiation to the cyst. To investigate this, cells were induced for encystation and a mixture of nonencysting and encysting cells was harvested at various time points (i.e., at 10 and 18 h postinduction [p.i.] of encystation) and labeled with CTXB (Fig. 3A). In trophozoites (Fig. 3A, image a), raft-like domains were found to be present in plasma and fla-

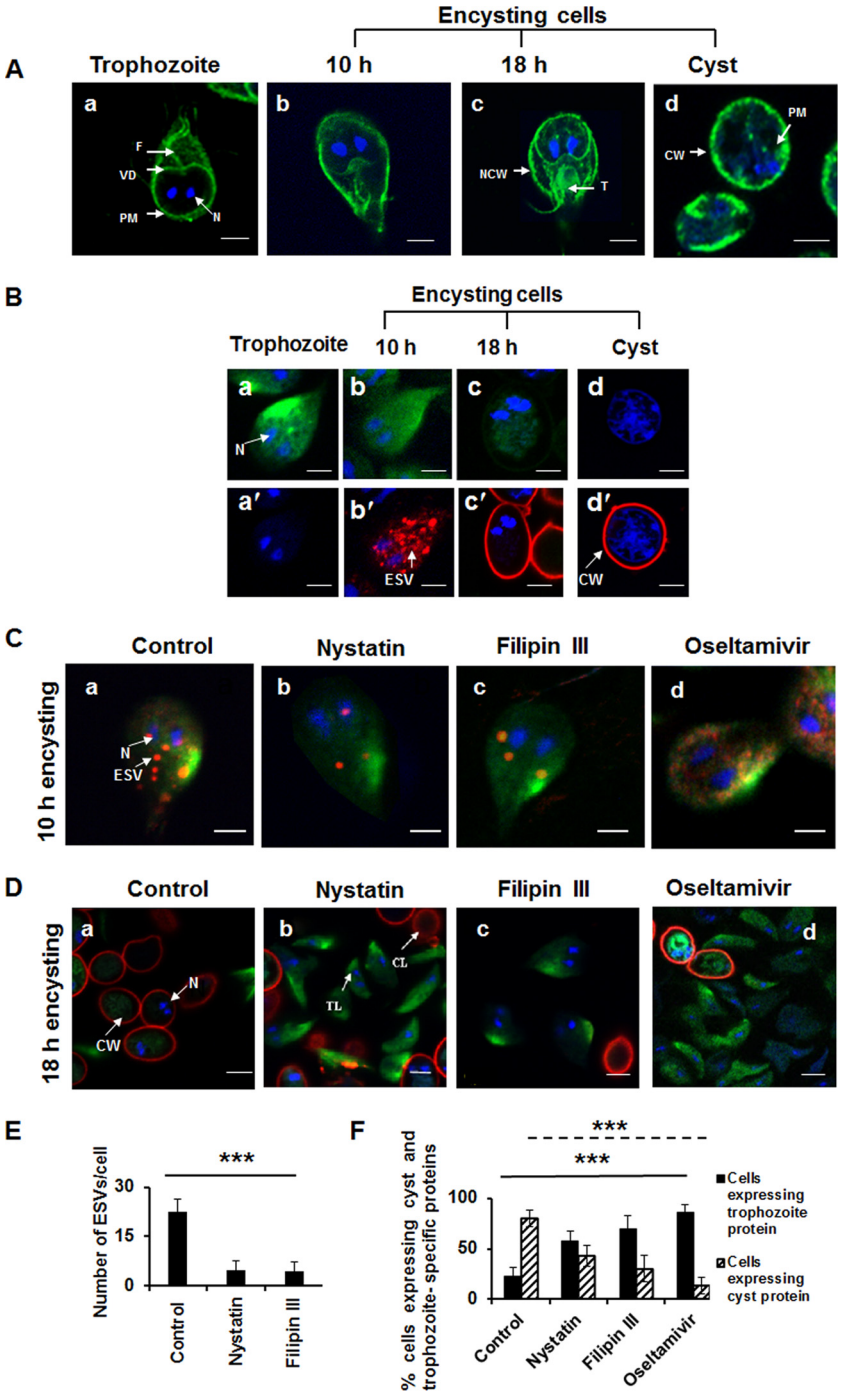


**FIG 3** Lipid rafts and encystation. (A) Expression of raft-like microdomains by encysting *Giardia*. (Image a) Nonencysting trophozoites; (image b) encysting cells at 10 h p.i. of encystation; (image c) encysting cells at 18 h p.i.; (image d) cysts. (B) Immunostaining of trophozoites, encysting cells, and cysts with trophozoite (green) and cyst (red) antibodies. (Images a and a′) Trophozoites; (images b and b′) encysting cells at 10 h p.i.; (images c and c′) encysting cells at 18 h p.i.; (images d and d′) cysts. (C) Effects of nystatin, filipin III, and oseltamivir on encysting cells at 10 h p.i. The encysting cells harvested at 10 h were labeled with trophozoite (green) and cyst (red) antibodies with or without inhibitors, as indicated. (Image a) Encysting cells at 10 h p.i. (control); (image b) nystatin (27 μM)-treated encysting cells; (image c) filipin III (7.6 μM)-treated encysting cells; (image d) oseltamivir (20 μM)-treated encysting cells. (D) Interruption of cyst production. Trophozoites were treated with inhibitors, subjected to encystation for 18 h, and labeled with cyst (red) and trophozoite (green) antibodies. (Image a) control; (image b) nystatin-treated encysting cells; (image c) filipin III-treated encysting cells; (image d) oseltamivir-treated encysting cells. (E) Assessing the number of ESVs produced by untreated and inhibitor-treated encysting cells. For ESV quantification, ~50 cells from 15 fields from 3 separate experiments were considered. (F) Quantitative determination of encysting cells at 18 h p.i. The percentages of control and inhibitor-treated *Giardia* cells expressing cyst and trophozoite proteins are shown. For quantification, ~200 cells from 9 fields from 3 separate experiments were counted. A one-way ANOVA followed by the Holm-Šídák method was used to calculate the *P* values. ***, $P < 0.001$. Solid line, *P* values for cells expressing trophozoite proteins; dashed line, *P* values for cells expressing cyst proteins. PM, plasma membrane; N, nucleus; VD, ventral disc; F, flagella; CW, cyst wall; NCW, nascent cyst wall; T, trophozoite; ESV, encystation-specific vesicle; TL, trophozoite-like structure; CL, cyst-like structure. Bars, 5 μm.

gellar membranes and the ventral disc. Rafts can be seen mostly in the plasma membranes in cells after 10 h p.i. (Fig. 3A, image b). Trophozoites harvested at 18 h p.i. (Fig. 3A, image c) displayed unique labeling of the nascent cyst walls, as well as the plasma membranes of encapsulated trophozoites. Interestingly, in cysts (Fig. 3A, image d), CTXB reactivity was observed in membranes beneath the cyst wall. Figure 3B demonstrates the staining patterns and specificities of the trophozoite (Troph-O-Glo) and cyst antibodies used in this study. It is clear that the expression of the trophozoite protein (green) decreased and that of the cyst protein (red) increased with the progression of encystation.

During the stage of differentiation from trophozoites to cysts, *Giardia* synthesizes small transport vesicles (known as encystation-specific vesicles [ESVs]) that transport the cyst wall protein to the membrane of this parasite and lay down the hardy cyst wall. Figure 3C shows the biogenesis of ESVs (red) by cells harvested at 10 h p.i. As shown, the number of ESVs was reduced significantly in nystatin- and filipin III-treated cells (Fig. 3C, images a to c). Interestingly, oseltamivir generated numerous small ESVs that were distributed throughout the cytoplasm (Fig. 3C, image d). Cells harvested at 18 h p.i. produced complete cysts, and the majority of these cysts expressed cyst proteins, which could be visualized by staining with cyst antibody (Fig. 3D, image a, red). The percentage of cysts decreased dramatically due to these inhibitors, as evidenced by the presence of more trophozoites (expressing green trophozoite proteins) than cysts (Fig. 3C, images a to d). The results of quantitative evaluations of inhibitor-treated cells expressing ESVs are shown in Fig. 3E. We do not show ESV expression data from oseltamivir-treated cells because they were extremely small and difficult to count. Figure 3F provides the results of a quantitative analysis of control and inhibitor-treated cells expressing trophozoite- and cyst-specific proteins.

To test if the disassembly of giardial raft-like microdomains affects the production of oval type I cysts (16), we examined the effects of these inhibitors on cyst morphologies. Figure 4A shows the dose-dependent effects of nystatin, filipin III, and oseltamivir on the morphological changes of giardial cysts. The control cysts in images a and a′ in Fig. 4A were found to be oval with uniform and refractive cyst walls and reacted mostly with cyst (red) rather than trophozoite (green) antibodies. Interestingly, nystatin (Fig. 4A, images b to f), filipin III (Fig. 4A, images b′ to f′), and oseltamivir (Fig. 4A, images b″ to f″) affected the cyst morphologies, yielding a mixture of round (with a smooth surface) and sometimes trophozoite-shaped water-resistant cells. These inhibitor-treated cysts also expressed trophozoite proteins (green) as opposed to mostly cyst proteins (red) (Fig. 4A, images f, f′, and f″). However, it is not known if these cysts were viable and competent to undergo excystation. The results of quantitation of classical (type I) and nonclassical (non-type I) cysts produced by controls and inhibitor-treated cells are depicted in Fig. 4B.

**Importance of cholesterol in the assembly of microdomains.** Cholesterol is an essential component of mammalian rafts, and it has been proposed that its depletion or sequestration disassembles microdomains (30, 31). Because we observed that nystatin and filipin III reduce CTXB and GM1 antibody staining, we wondered if changes in the amount of cholesterol influence raft assembly by *Giardia*. To test this possibility, trophozoites were cultured in Diamond's TYI-S-33 medium (16) supplemented with bovine bile (0.5 mg/ml) and dialyzed fetal bovine serum (DFBS; 5%) instead of adult bovine serum (ABS; 5%). The purpose of using DFBS was to culture parasites in a medium containing reduced amounts of cholesterol, as we speculated that lowering the amount of free cholesterol should facilitate the binding of nystatin and filipin III with raft microdomains (which are not hindered by excess cellular and environmental cholesterol) and a greater effect on the disassembly of microdomains would be observed. The DFBS used in this study was purchased from Gibco Invitrogen (Carlsbad, CA) and was free of molecules with molecular weights below 10,000 (i.e., lipophilic molecules, hormones, peptides cytokines, glucose, and amino acids). To further test if the DFBS contained a reduced amount of cholesterol, we measured the amount of cholesterol in DFBS and compared the amount with that in ABS using a cholesterol assay kit (Invitrogen). Figure 5A shows that DFBS contains ~38% less cholesterol than ABS (5.0 ng/mg versus 8.1 ng/mg protein). Trophozoites cultured in a medium containing DFBS also contain 40 to 45% less cholesterol than parasites grown in ABS-supplemented medium. However, the reduction of cholesterol did not change the growth or replication of the trophozoites (see the growth curve in Fig. 5B).

Next, we wondered if trophozoites cultured in a DFBS-containing medium were capable of assembling raft domains such as trophozoites cultured in an ABS-supplemented medium, as shown in Fig. 1 and 2. Figure 5C shows the labeling of giardial microdomains in trophozoites by Alexa Fluor 488-conjugated CTXB. Although CTXB reacted with membranes, flagella, and ventral discs, the overall labeling intensity was lower than that for trophozoites cultured in ABS (Fig. 5C, images a and b). Furthermore, all three inhibitors (i.e., nystatin, filipin III, and oseltamivir) inhibited CTXB labeling completely, as depicted in Fig. 5C, images c to e. Likewise, the intensity of GM1 labeling (using GM1 antibody) was also low in trophozoites cultured in DFBS-containing medium (Fig. 5C, images a′ and b′). We found that these three inhibitors either reduced or altered the pattern of staining with GM1 antibody, as shown in Fig. 5D and E.

It was also examined if reduced cholesterol interferes with encystation and cyst production. *Giardia* trophozoites cultured in Diamond's TYI-S-33 medium containing DFBS were subjected to encystation in the presence and absence of nystatin, filipin III, or oseltamivir for 10 and 18 h. Encysting trophozoites were harvested, fixed, and dually labeled with cyst and trophozoite (Troph-O-Glo) antibodies, as described in Materials and Methods. Figure 6A (images a to d) demonstrates that culturing of cells in DFBS-containing medium reduces the CTXB labeling of nonencysting and encysting trophozoites as well as that of cysts. The biogenesis of ESVs by encysting cells cultured in DFBS-supplemented medium (10 h p.i. of encystation) resulted in the production of numerous small vesicles, compared with cells encysted in ABS-containing medium (Fig. 6B, images a and b). As expected, ESV biogenesis was further reduced when encystation was carried out in the presence of inhibitors in DFBS medium (Fig. 6B, images b to e). Figure 6C (image b) shows that at 18 h, DFBS-supplemented encystation medium produced fewer cysts than ABS-containing medium (image a) that could be stained with cyst antibody. The number of cells expressing trophozoite proteins (green) was also higher in DFBS cysts than in ABS cysts. Nystatin, filipin III, and oseltamivir interfered with cyst production, as evidenced by green trophozoite antibody staining (Fig. 6C, images b to e). The percentage of cells expressing trophozoite and cyst proteins by 18 h p.i. is shown in Fig. 6D.

**Cholesterol supplementation experiments.** The experiments

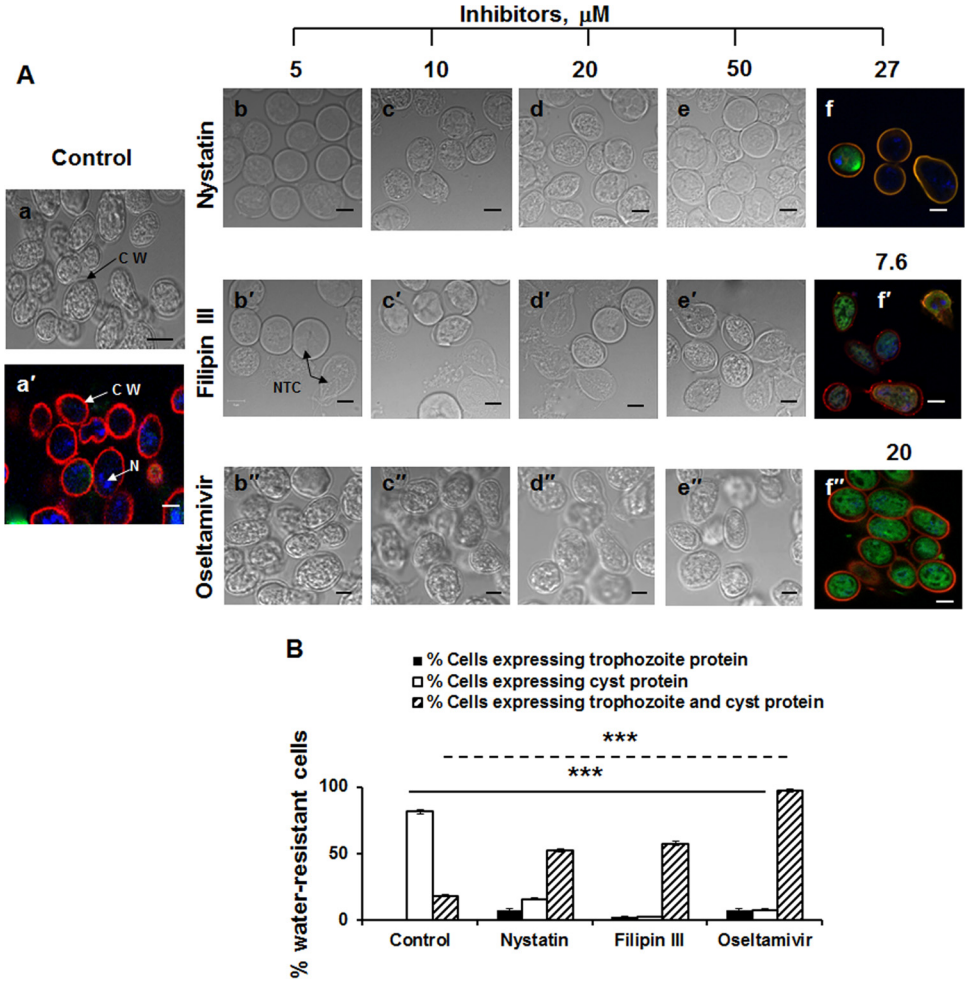


**FIG 4** Disruption of microdomains alters cyst morphology. (A) Effects of nystatin, filipin III, and oseltamivir. (Image a) Differential inference contrast picture of water-resistant cysts; (image a′) cysts labeled with both cyst and trophozoite antibodies; (images b to e) effects of various concentrations of nystatin (5 to 50 μM) on cysts; (image f) nystatin (27 μM) induces the expression trophozoite proteins (green) side-by-side with cyst proteins (red), unlike the typical cysts shown in image a′; (images b′ to e′) filipin III (5 to 50 μM) alters the morphology of cysts, producing round, nontypical cysts comparable to those produced by nystatin-treated cells; (image f′) filipin III (7.6 μM) triggers the expression of both trophozoite-specific (green) and cyst-specific (red) proteins; (images b″ to e″) effects of oseltamivir (5 to 50 μM) on cyst morphology. Oseltamivir (20 μM) also induces the expression of trophozoite proteins (green) along with cyst proteins (red) (image f″). CW, cyst wall; NTC, nontypical cysts; N, nucleus stained with DAPI. Bars, 5 μm. (B) Quantitative assessment of cysts expressing only trophozoite proteins, only cyst proteins, or both trophozoite and cyst proteins. For quantification, ~100 cells from 9 randomly selected fields from 3 separate experiments were counted. The results are means ± SDs. The significance was analyzed by one-way ANOVA followed by the Holm-Šídák method. ***, $P < 0.001$. Solid line, *P* values for cells expressing cyst proteins; dashed line, *P* values for cells expressing trophozoite and cyst proteins.

described above indicated that although culturing of *Giardia* in DFBS-supplemented medium (containing 30 to 40% less cholesterol than ABS medium) did not affect the growth of trophozoites, it affected the assembly of microdomains and interfered with the encystation process. To investigate this finding further, we carried out a cholesterol supplementation experiment as described in Materials and Methods. *Giardia* trophozoites were cultured in DFBS-containing medium and subjected to encystation for 18 h in the presence or absence of 215 μg/ml of cholesterol, as described in Materials and Methods. Cells were harvested by centrifugation and kept in water overnight at 4°C before labeling with cyst and trophozoite antibodies. Compared with the findings for cysts obtained from ABS-supplemented medium (Fig. 7A, image a), the majority (~65%) of cysts obtained from DFBS-supplemented medium cross-reacted with trophozoite antibody (Fig. 7A, image b, green). The addition of cholesterol in DFBS-supplemented medium rescued the affected cysts significantly, as evidenced by the reaction with cyst antibody (Fig. 7A, image c). Because nystatin and filipin III are cholesterol-binding agents, we thought that cholesterol supplementation should also neutralize the effects of nystatin and filipin III. It was observed that although the reversal effects of cholesterol on nystatin-induced changes were more prominent than those on filipin III-induced changes (Fig. 7A, images d and e), none of these differences were statistically significant (Fig. 7B). The percentage of cells representing trophozoite and cyst-like structures is shown in Fig. 7B.

**Isolation of cholesterol- and GM1-enriched microdomains from trophozoites.** Our microscopic results (Fig. 1 to 6) strongly support the idea that lipid rafts are assembled by *Giardia* and can be identified by immunostaining with CTXB and GM1 antibodies. Therefore, to validate the microscopic data, we isolated giardial rafts by OptiPrep gradient flotation as described in Materials and

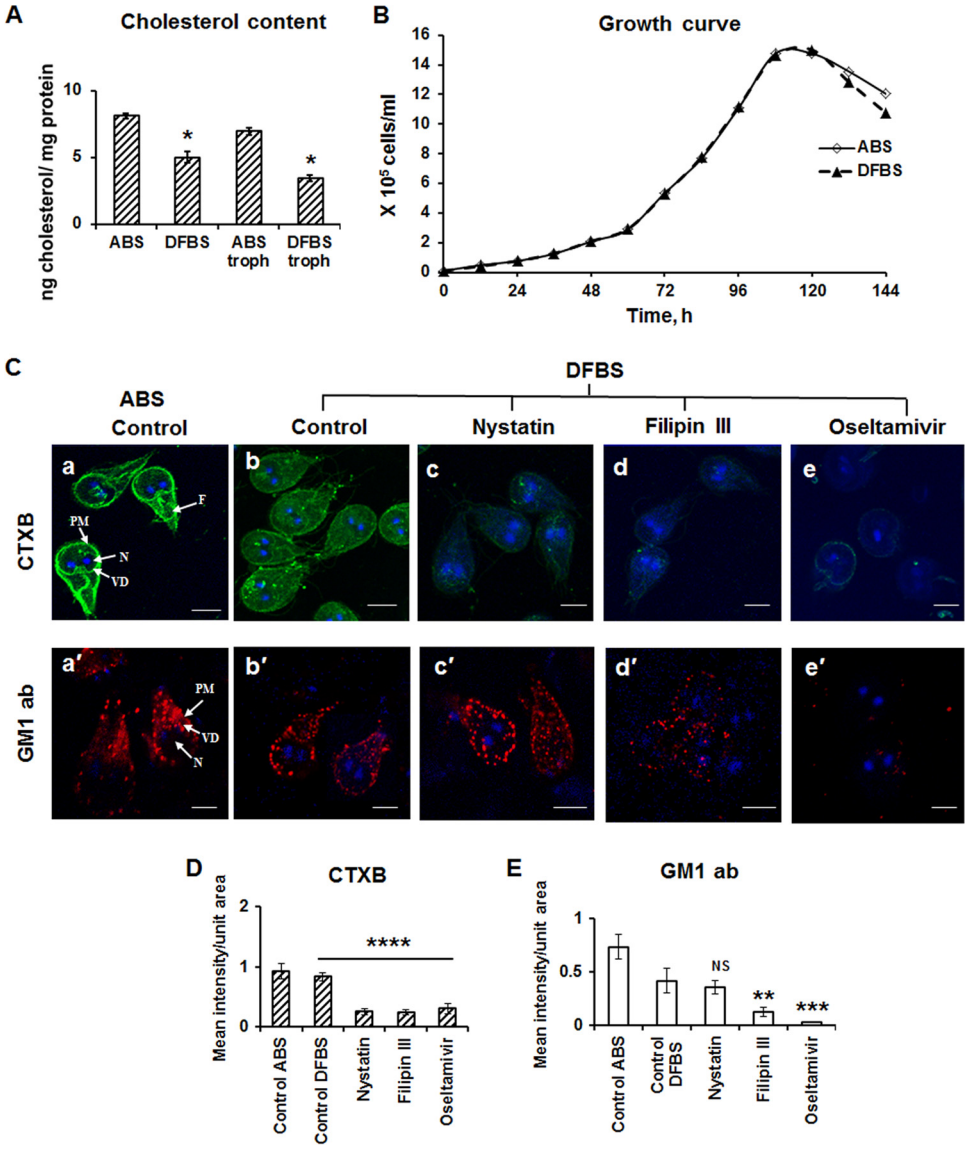


**FIG 5** (A) Measuring cholesterol in ABS, DFBS, and trophozoites (troph) cultured in ABS- or DFBS-supplemented medium using an Amplex red cholesterol assay kit (Invitrogen). *, $P < 0.05$, as analyzed by Student's *t* test. (B) Growth curve. Trophozoites were cultured in Diamond's TYI-S-33 medium supplemented with either ABS or DFBS, and their growth was measured. (C) Effects of inhibitors on CTXB antibodies (green; images b to e) and GM1 antibodies (red; b′ to e′) on trophozoites cultured in DFBS-supplemented medium. (Images a and a′) Trophozoites grown in ABS-supplemented growth medium. Nuclei were stained with DAPI. N, nucleus; PM, plasma membrane; F, flagella; VD, ventral disc. Bars, 5 μm. (D and E) Quantitative measurements of CTXB (D) and GM1 (E) antibody labeling of control and inhibitor-treated trophozoites cultured in DFBS. The staining of trophozoites cultured in ABS-supplemented medium is also shown. For image analyses (fluorescence intensities), approximately 50 cells were selected from 9 to 18 fields from 3 to 4 experiments and analyzed by Zeiss Zen 2009 software. The significance was analyzed by one-way ANOVA. *P* values shown in panel D and E were calculated by the Holm-Šídák method by comparison of the results for the treatment groups with those for the group treated with control DFBS. **, $P < 0.01$; ***, $P < 0.001$; ****, $P < 0.0001$; NS, not significant.

Methods. Briefly, trophozoites (control trophozoites and nystatin- and oseltamivir-treated trophozoites) were mixed with CTXB-HRP solution (19, 20), washed, solubilized in a buffer containing 1% Triton X-100, and subjected to OptiPrep gradient centrifugation. The fractions were isolated, and CTXB-HRP-enriched LR fractionations were identified by ELISA using a chemiluminescent reagent. To identify cholesterol-enriched fractions, cells (without conjugated CTXB-HRP) were solubilized in 1% Triton X-100, followed by OptiPrep gradient centrifugation. Cholesterol-enriched fractions were identified using an Amplex red cholesterol assay kit. Two cholesterol peaks were observed. One peak was found in the upper part (fractions 2 to 5) and another one was found in the lower region (fraction 7) of the gradient (Fig. 8A). It was noted that GM1- and cholesterol-enriched raft-like microdomains (fractions 2 to 5) float to the upper gradient fractions and are altered by nystatin and oseltamivir (Fig. 8B), as evidenced by the dispersed pattern of separation caused by the inhibitors. The sensitivity of peak 1 to nystatin and oseltamivir suggested that GM1- and cholesterol-enriched raft domains are likely the major lipid rafts in *Giardia* and participate in the encystation process. On the contrary, the cholesterol peak at fraction 7 (Fig. 8C) was not significantly affected by these inhibitors, indi-

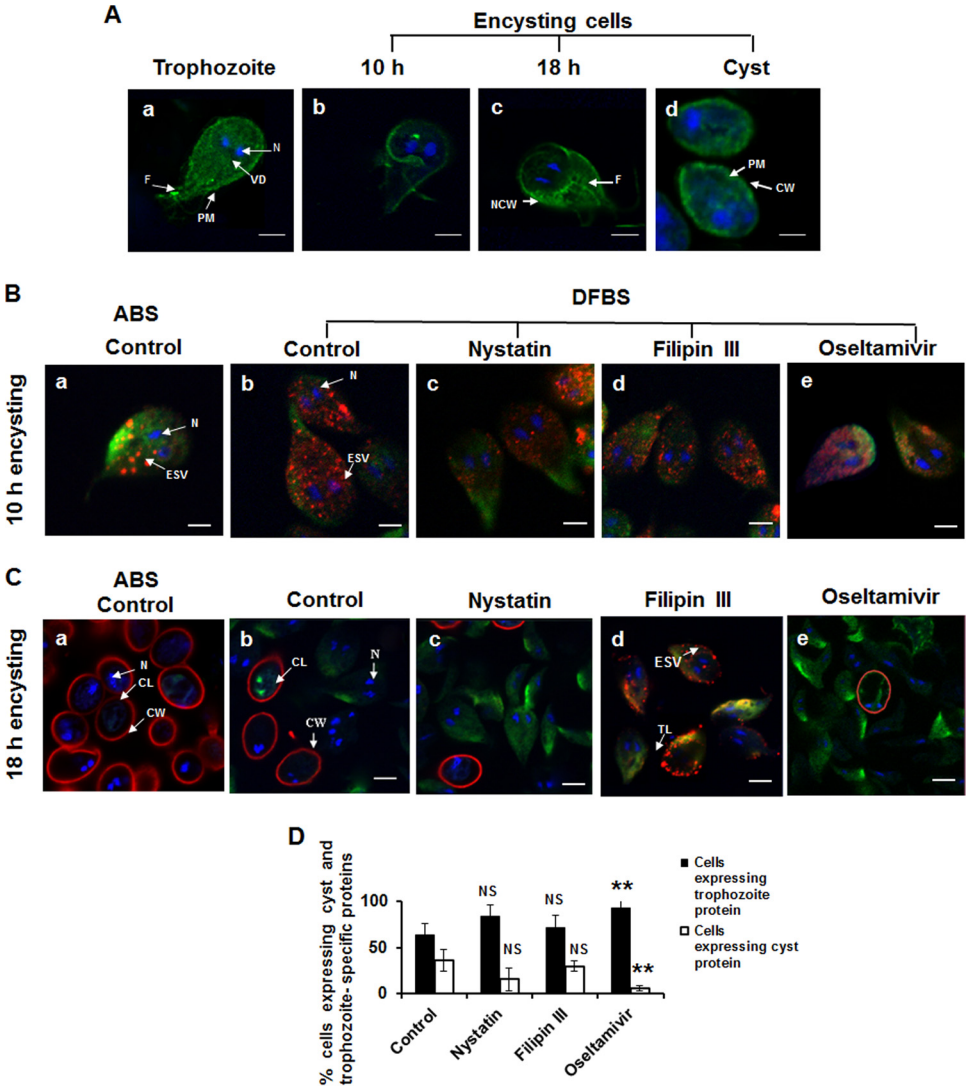


**FIG 6** (A) Expression of raft-like microdomains by encysting *Giardia* cultured in 5% DFBS-containing medium. The cells were labeled with Alexa Fluor 488-conjugated CTXB and DAPI and viewed under a confocal microscope. (Image a) Nonencysting trophozoites; (image b) encysting cells at 10 h p.i. of encystation; (image c) encysting cells at 18 h p.i. of encystation; (image d) water-resistant cysts. (B) ESV biogenesis and expression of trophozoite proteins. Encysting cells at 10 h p.i. of encystation (control and inhibitor treated) were labeled with trophozoite (green) and cyst (red) antibodies as described in Materials and Methods. (Image a) Labeling of encysting cells at 10 h p.i. of encystation in medium supplemented with ABS; (image b) encysting trophozoites at 10 h p.i. of encystation differentiated in medium containing DFBS; (image c) nystatin (27 μM) treatment; (image d) filipin III (7.6 μM) treatment; (image e) oseltamivir (20 μM) treatment. (C) Induction of encystation in DFBS-supplemented medium affects cyst production. Control and inhibitor-treated trophozoites were allowed to encyst for 18 h before labeling with cyst (red) and trophozoite (green) antibodies. (Image a) Cyst antibody-labeled water-resistant cysts produced in ABS-supplemented medium; (image b) cysts generated in ABS-supplemented medium; (image c) nystatin (27 μM) treatment; image d, filipin III (7.6 μM) treatment; image e, oseltamivir (20 μM) treatment. N, nucleus; ESV, encystation-specific vesicle; PM, plasma membrane; N, nucleus; VD, ventral disc; F, flagella; CW, cyst wall; NCW, nascent cyst wall; CL, cyst-like structure; TL, trophozoite-like structure. Bars, 5 μm. (D) Quantitative estimates of water-resistant cells expressing trophozoite proteins or cyst proteins. For quantification, 125 cells from 6 randomly selected fields from 2 separate experiments were counted. Data were analyzed by a one-way ANOVA followed by the Holm-Šídák method. **, $P < 0.01$; NS, not significant.

cating that the second peak could be a non-raft-associated cholesterol-enriched fraction.

## DISCUSSION

In this study, we show for the first time that *Giardia* has the ability to assemble cholesterol- and GM1 ganglioside-enriched raft-like domains, which can be identified by labeling with fluorescently conjugated CTXB and GM1 antibodies. A general lipid-staining dye (i.e., FAST Dil oil) was used to distinguish raft and non-raft lipids in *Giardia* (18). The results of our experiments suggest that while CTXB and GM1 antibody labels are specific for raft domains, FAST Dil oil distinctly stains cytoplasmic and endoplasmic reticulum membrane lipids (Fig. 1).

Since cholesterol is an essential component of membrane microdomains in the majority of eukaryotic cells, we asked if giardial microdomains also contain cholesterol and whether the removal of cholesterol from microdomains disintegrates their structures and functions. Two strategies were followed to address this issue. In strategy I, parasites were treated with cholesterol-binding agents—e.g., nystatin and filipin III—followed by labeling with

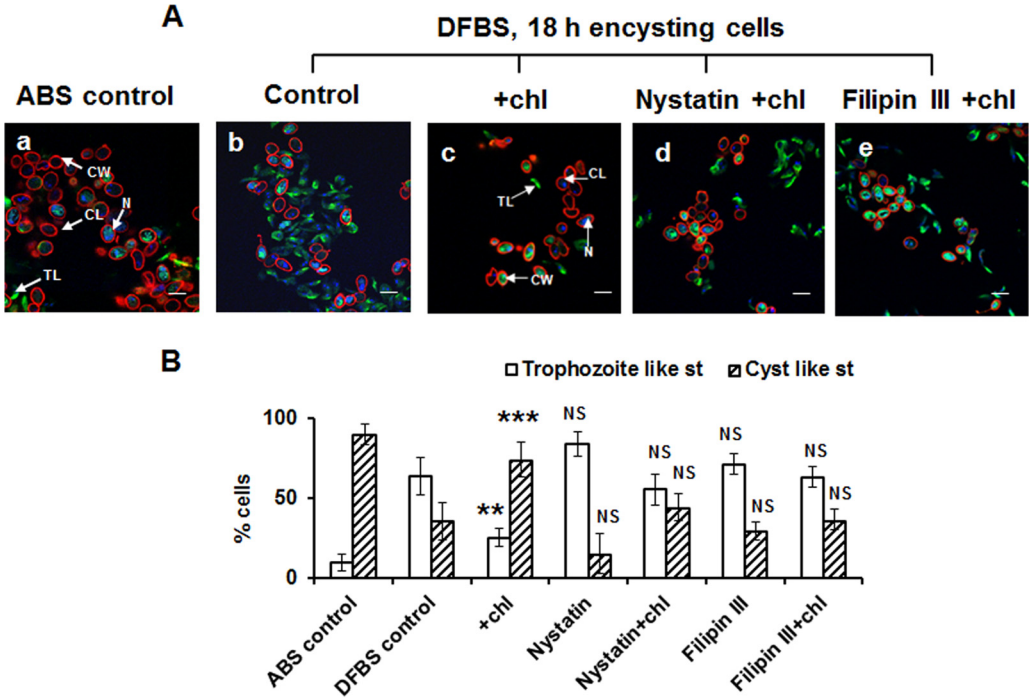


**FIG 7** Cholesterol supplementation induces encystation in *Giardia* cells cultured in DFBS-supplemented medium. (A) (Images a and b) Cysts generated in ABS- and DFBS-containing medium, respectively. Cysts were harvested, kept in water (4°C) overnight, and stained with trophozoite and cyst antibodies. (Image c) Cholesterol (chl; 215 μg/ml) supplementation of DFBS-containing encystation (18 h) medium. (Images d and e) Cysts treated with nystatin plus cholesterol and filipin III plus cholesterol, respectively. N, nucleus; PM, plasma membrane; VD, ventral disc; CW, cyst wall; TL, trophozoite-like structure; CL, cyst-like structure. Bars, 5 μm. (B) Quantitation of trophozoite-like and cyst-like structures (st) that were produced in medium supplemented with small amounts of cholesterol under the influence of nystatin and filipin III. For quantitation, 75 cells from 9 fields from 3 separate experiments were counted. Calculations of significance were carried out by comparing the results for the treatments with those for the DFBS control, and the data were analyzed by one-way ANOVA followed by the Holm-Šídák method. **, $P < 0.01$; ***, $P < 0.001$; NS, not significant.

CTXB and GM1 antibodies. The polyene antibiotics, including nystatin and filipin III, are commonly used as raft inhibitors to disrupt sterol-containing lipid rafts in eukaryotic cells. Absorption and fluorescence studies have indicated that in the presence of cholesterol or ergosterol, polyene antibiotics form aggregates (called polyene aggregates) and thereby affect the orderly structured steroid molecules within the microdomains (32). We found that both nystatin and filipin III disrupt membrane rafts in trophozoites (Fig. 2). Nystatin and filipin III also inhibit the synthesis of encystation-specific vesicles (ESVs) (Fig. 3), which are secretory vesicles that are synthesized at the onset of encystation and transport cyst wall proteins to plasma membranes for constructing osmosis-resistant cyst walls (33). Nystatin- and filipin III-treated cysts express trophozoite proteins rather than cyst proteins and generate fewer cysts with an altered morphology (Fig. 4). However, it will be interesting to see if these inhibitor-treated cysts are viable and morphologically transform into trophozoites (i.e., undergo excystation). The goal of strategy II was to culture *Giardia* in a medium containing reduced amounts of cholesterol and examine the microdomain assembly. Because serum is the major source of cholesterol for *Giardia*, we thought that the replacement of ABS with DFBS—which contains 30 to 40% less cholesterol than ABS (Fig. 5A and B)—would allow us to assess the role of cholesterol in microdomain assembly. In the laboratory, *Giardia* is cultured in Diamond's TYI-S-33 medium and supplemented with serum and bovine bile, which are the major sources of cholesterol for trophozoites (34). Cholesterol and cholesteryl ester concentrations are different in growth and encystation medium containing small and large amounts of bile (11). In the study described in this paper, we used an encystation medium (17) that contained DFBS instead of ABS and that was supplemented with a large amount of bile (5 mg/ml bovine bile). DFBS contains 30 to 40% less cholesterol than ABS, and this decrease is sufficient to affect raft formation and encystation (Fig. 5). The addition of a small amount of cholesterol (215 μg/ml, ~21%) reverses the process by resulting in the production of type I cysts (Fig. 7). These observations support the idea that cholesterol is an important component of giardial membrane microdomains and interruption of cholesterol assimilation in microdomains—by either inhibitor treatment or culturing of parasites in medium containing a small amount of cholesterol—inhibits raft formation. Like inhibitors, cholesterol reduction also affects ESV biogenesis and cyst production (Fig. 5 and 6). The number of cysts increases when cholesterol is added to the encystation medium (Fig. 7), indicating that cholesterol is important for raft assembly and encystation.

Lujan et al. (35) reported that cholesterol starvation induces encystation. In that study, the authors cultured trophozoites in TYI-S-33 medium supplemented with 10% ABS (a cholesterol-enriched condition) before they were transferred to encystation medium supplemented with lipoprotein-deficient serum (LPDS), which is low in cholesterol. Based on the findings obtained under these conditions, Lujan et al. (35) proposed that cholesterol starvation triggers encystation. In the current study, we initially used ABS followed by encystation in medium with a large amount of

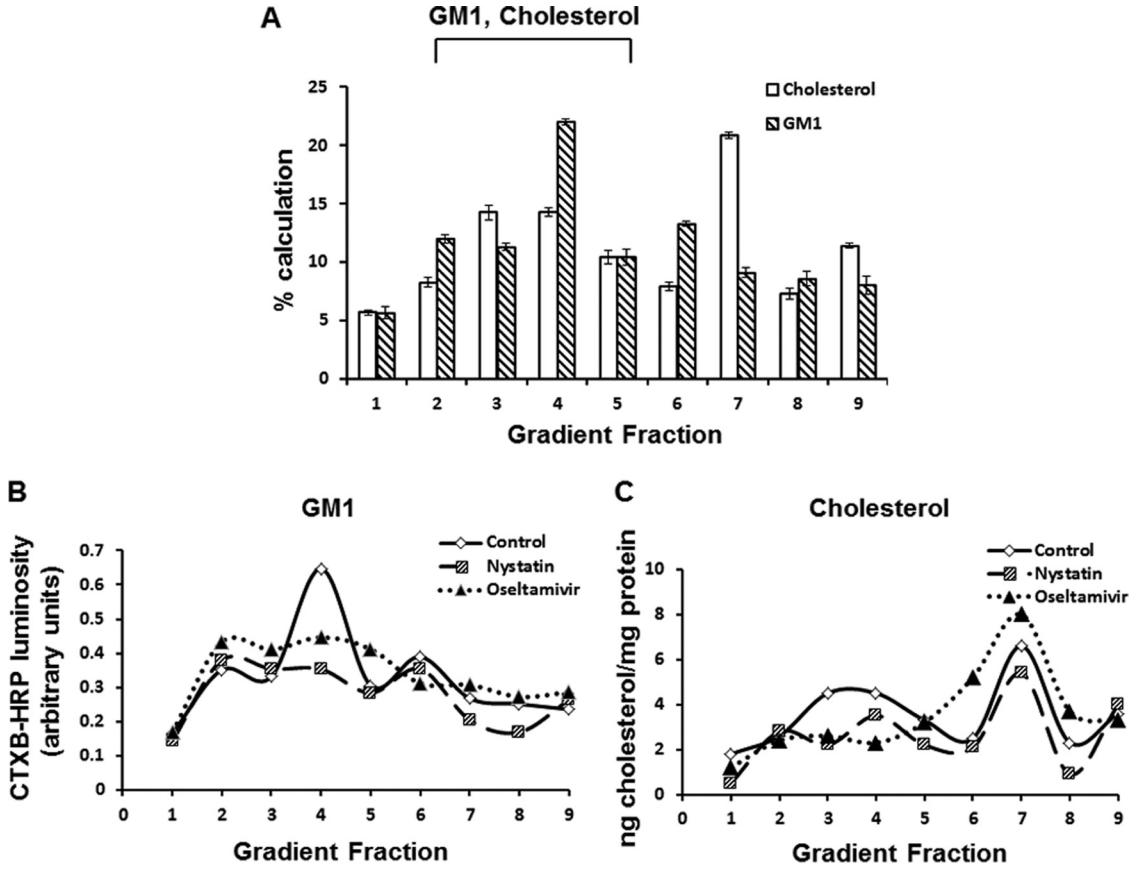


**FIG 8** Isolation of GM1- and cholesterol-enriched lipid rafts. To isolate GM1-enriched microdomains, control and inhibitor-treated *Giardia* trophozoites were labeled with CTXB-HRP, lysed in 1% Triton X-100 buffer, and subjected to OptiPrep gradient ultracentrifugation. To identify cholesterol-enriched microdomains, trophozoites not labeled with CTXB-HRP were used. Fractions (1 ml) were collected from the top of the gradients, and the abundances of GM1 and cholesterol were measured by ELISAs. (A) The percentages of total cholesterol and GM1 appearing in each fraction are shown. Values are representative of those from 2 separate experiments (carried out in duplicate) performed on different days with different batches of cells and treatments. Fractions 2 to 5 are considered GM1 and cholesterol enriched, whereas fraction 7 is probably non-raft associated. (B and C) Nystatin and oseltamivir alter the distribution patterns of GM1 (B) and cholesterol (C). Results represent the means from 2 separate experiments carried out in duplicate.

bile, which could be blocked by nystatin and filipin III (two cholesterol-binding agents and LR inhibitors) (Fig. 2). To better understand the role of cholesterol and raft domains in encystation, trophozoites were cultured in medium containing 5% DFBS (which is low in cholesterol compared to the amount in ABS; Fig. 5), followed by encystation. We found that DFBS-supplemented medium inhibited raft assembly as well as encystation. Interestingly, addition of cholesterol induced LR assembly and restored encystation. Thus, our results clearly suggest that an adequate amount of cholesterol is required for maintaining the integrity of raft-like domains, which is critical for encystation. We speculate that at the onset of encystation, encystation stimuli activate proteins/molecules that are partitioned in microdomains and initiate the encystation process. It is possible that once the encystation is initiated, rafts are no longer required and encystation may continue without cholesterol (under cholesterol-starved conditions), as observed previously (35, 36).

Since oseltamivir inhibits both the neuronal levels of GM1 and morphine-induced hyperalgesia in mice (25), we wondered if this inhibitor could also be used as a raft disruptor and a blocker of encystation and cyst production. We found that oseltamivir indeed blocks raft assembly, ESV biogenesis, and the formation of type I cysts (Fig. 2 to 7). However, the mechanism of oseltamivir action in *Giardia* is not clear. So far, no putative sequences of sialidase (neuraminidase) or GM1 synthase are annotated in the *Giardia* Genome Database (www.GiardiaDB.org). Reports suggest that oseltamivir exhibits limited inhibitory effects on human sialidase. Hata et al. (37) have reported that oseltamivir is not effective in blocking the human enzyme (i.e., sialidase), even at a 1 mM concentration, when they used recombinant human sialidases. On the other hand, the same inhibitor reduced viral neuraminidase activity when it was used at nanomolar levels. Thus, it appears that the oseltamivir action is more specific for viral neuraminidase than for mammalian sialidase. Morimoto et al. (38) suggested that oseltamivir is a substrate for P glycoprotein and its distribution in the brain depends on P glycoprotein function. *Giardia* growth medium contains lipids and gangliosides (T. T. Duarte, personal communication), and since this parasite is unable to synthesize its own lipids *de novo* (5, 8, 11), it is likely that the majority of GM1 lipids that are present in giardial rafts is likely to be taken up from the medium via a specific transport system/pathway which also binds with oseltamivir. In fact, several putative P glycoproteins (also known as multidrug-resistant proteins or ATP-binding cassettes) are present in *Giardia* (www.Giardia

DB.org) and could be involved in GM1 and oseltamivir internalization. In the future, it will be important to determine if oseltamivir and GM1 gangliosides compete for the same transporters and if overexpression of these transporters makes *Giardia* susceptible to oseltamivir.

We were also successful in isolating membrane microdomains from *Giardia* trophozoites by density gradient centrifugation (Fig. 8). The GM1- and cholesterol-enriched lipid rafts migrate toward the top of the gradient in the upper fractions (Fig. 8A, fractions 2 to 5). Earlier reports have indicated that GM1- and cholesterol-enriched microdomains isolated from mammalian and parasitic cells also migrate to the upper to middle fractions of the gradient (19, 20, 39). It was observed that both nystatin and oseltamivir disrupt GM1- and cholesterol-enriched microdomains (Fig. 8B and C). This observation further supports our microscopic data indicating that GM1- and cholesterol-enriched membrane microdomains are present in this parasite and can be disrupted by cholesterol-binding agents and oseltamivir. In addition to a GM1- and cholesterol-enriched fraction, another peak that contained large amounts of cholesterol and small amounts of GM1 that migrated to lower fractions (Fig. 8, fraction 7) of the gradient was identified. The second cholesterol-enriched microdomains could be associated with non-lipid raft membranes, tightly associated with a cytoskeleton component, and involved in cytoskeleton remodeling and function (20). However, more in-depth experiments are required to support this hypothesis.

An investigation conducted more than 5 decades ago revealed that the antifungal drug nystatin exhibits strong giardiacidal activity (40). Our studies indicate that nystatin could exert its antigiardial activity by disrupting the raft-like microdomains present in *Giardia*. We propose that giardial rafts should be considered potential targets in the development of new therapies against this waterborne pathogen in the future.

## ACKNOWLEDGMENTS

We thank Igor Almeida for stimulating discussion and Armando Varela for helping us with microscopy experiments, as well as Leobarda Robles-Martinez for commenting on the manuscript. We are also thankful to Christiancel Salazar for technical help during the course of this investigation.

The biochemical and confocal microscopy analyses were carried out at the Biomolecule Analysis and Cytometry, Screening, and Imaging Facility as well as the Genomic Core Facility at the Border Biomedical Research Center (UTEP), supported by a grant (G12MD007592) from NIMHD (NIH). This work was partially supported by a grant (R01AI 095667) from NIAID (NIH) to S.D.

## REFERENCES

1. **Hunter PR, Thompson RC.** 2005. The zoonotic transmission of *Giardia* and *Cryptosporidium*. Int J Parasitol **35:**1181–1190. http://dx.doi.org/10.1016/j.ijpara.2005.07.009.
2. **Wolfe MS.** 1992. Giardiasis. Clin Microbiol Rev **5:**93–100.
3. **Adam R.** 2001. Biology of *Giardia lamblia*. Clin Microbiol Rev **14:**447–475. http://dx.doi.org/10.1128/CMR.14.3.447-475.2001.
4. **Roxström-Lindquist K, Palm D, Reiner D, Ringqvist E, Svärd SG.** 2006. *Giardia* immunity—an update. Trends Parasitol **22:**26–31. http://dx.doi.org/10.1016/j.pt.2005.11.005.
5. **Yichoy M, Duarte TT, De Chatterjee A, Mendez TL, Aguilera KY, Roy D, Roychowdhury S, Aley SB, Das S.** 2011. Lipid metabolism in *Giardia*: a post-genomic perspective. Parasitology **138:**267–278. http://dx.doi.org/10.1017/S0031182010001277.
6. **Reiner DS, Wang CS, Gillin FD.** 1986. Human milk kills *Giardia lamblia* by generating toxic lipolytic products. J Infect Dis **154:**825–832. http://dx.doi.org/10.1093/infdis/154.5.825.
7. **Das S, Reiner DS, Zenian J, Hogan DL, Koss MA, Wang CS, Gillin FD.** 1988. Killing of *Giardia lamblia* trophozoites by human intestinal fluid in vitro. J Infect Dis **157:**1257–1260. http://dx.doi.org/10.1093/infdis/157.6.1257.
8. **Jarroll EL, Muller PJ, Meyer EA, Morse SA.** 1981. Lipid and carbohydrate metabolism of *Giardia lamblia*. Mol Biochem Parasitol **2:**187–196. http://dx.doi.org/10.1016/0166-6851(81)90099-2.
9. **Farthing MJ, Keusch GT, Carey MC.** 1985. Effects of bile and bile salts on growth and membrane lipid uptake by *Giardia lamblia*. Possible implications for pathogenesis of intestinal disease. J Clin Invest **76:**1727–1732.
10. **Gibson GR, Ramirez D, Maier J, Castillo C, Das S.** 1999. *Giardia lamblia*: incorporation of free and conjugated fatty acids into glycerol-based phospholipids. Exp Parasitol **92:**1–11. http://dx.doi.org/10.1006/expr.1999.4389.
11. **Ellis JE, Wyder MA, Jarroll EL, Kaneshiro ES.** 1996. Changes in lipid composition during in vitro encystation and fatty acid desaturase activity of *Giardia lamblia*. Mol Biochem Parasitol **81:**13–25. http://dx.doi.org/10.1016/0166-6851(96)02677-1.
12. **Das S, Castillo C, Stevens T.** 2001. Phospholipid remodeling/generation in *Giardia*: the role of the Lands cycle. Trends Parasitol **17:**316–319. http://dx.doi.org/10.1016/S1471-4922(01)01901-8.
13. **Mendez TL, De Chatterjee A, Duarte TT, Gazos-Lopes F, Robles-Martinez L, Roy D, Sun J, Maldonado RA, Roychowdhury S, Almeida IC, Das S.** 2013. Glucosylceramide transferase activity is critical for encystation and viable cyst production by an intestinal protozoan, *Giardia lamblia*. J Biol Chem **288:**16747–16760. http://dx.doi.org/10.1074/jbc.M112.438416.
14. **Diamond LS, Harlow DR, Cunnick CC.** 1978. A new medium for the axenic cultivation of *Entamoeba histolytica* and other *Entamoeba*. Trans R Soc Trop Med Hyg **72:**431–432. http://dx.doi.org/10.1016/0035-9203(78)90144-X.
15. **Keister DB.** 1983. Axenic culture of *Giardia lamblia* in TYI-S-33 medium supplemented with bile. Trans R Soc Trop Med Hyg **77:**487–488. http://dx.doi.org/10.1016/0035-9203(83)90120-7.
16. **Gillin FD, Boucher SE, Rossi SS, Reiner DS.** 1989. *Giardia lamblia*: the roles of bile, lactic acid, and pH in the completion of the life cycle in vitro. Exp Parasitol **69:**164–174. http://dx.doi.org/10.1016/0014-4894(89)90185-9.
17. **Kane AV, Ward HD, Keusch GT, Pereira ME.** 1991. In vitro encystation of *Giardia lamblia*: large-scale production of in vitro cysts and strain and clone differences in encystation efficiency. J Parasitol **77:**974–981. http://dx.doi.org/10.2307/3282752.
18. **Laughlin RC, McGugan GC, Powell RR, Welter BH, Temesvari LA.** 2004. Involvement of raft-like plasma membrane domains of *Entamoeba histolytica* in pinocytosis and adhesion. Infect Immun **72:**5349–5357. http://dx.doi.org/10.1128/IAI.72.9.5349-5357.2004.
19. **Graham JM.** 2002. Purification of lipid rafts from cultured cells. Sci World J **2:**1662–1666. http://dx.doi.org/10.1100/tsw.2002.846.
20. **Blank N, Gabler C, Schiller M, Kriegel M, Kalden JR, Lorenz HM.** 2002. A fast, simple and sensitive method for the detection and quantification of detergent-resistant membranes. J Immunol Methods **271:**25–35. http://dx.doi.org/10.1016/S0022-1759(02)00335-6.
21. **Stefanić S, Spycher C, Morf L, Fabrias G, Casas J, Schraner E, Wild P, Hehl AB, Sonda S.** 2010. Glucosylceramide synthesis inhibition affects cell cycle progression, membrane trafficking, and stage differentiation in *Giardia lamblia*. J Lipid Res **51:**2527–2545. http://dx.doi.org/10.1194/jlr.M003392.
22. **Nguyen DH, Hildreth JE.** 2000. Evidence for budding of human immunodeficiency virus type 1 selectively from glycolipid-enriched membrane lipid rafts. J Virol **74:**3264–3272. http://dx.doi.org/10.1128/JVI.74.7.3264-3272.2000.
23. **Puri V, Watanabe R, Singh RD, Dominguez M, Brown JC, Wheatley CL, Marks DL, Pagano RE.** 2001. Clathrin-dependent and -independent internalization of plasma membrane sphingolipids initiates two Golgi targeting pathways. J Cell Biol **154:**535–547. http://dx.doi.org/10.1083/jcb.200102084.
24. **Pohl J, Ring A, Stremmel W.** 2002. Uptake of long-chain fatty acids in HepG2 cells involves caveolae: analysis of a novel pathway. J Lipid Res **43:**1390–1399. http://dx.doi.org/10.1194/jlr.M100404-JLR200.
25. **Crain SM, Shen KF.** 2004. Neuraminidase inhibitor, oseltamivir blocks GM1 ganglioside-regulated excitatory opioid receptor-mediated hyperalgesia, enhances opioid analgesia and attenuates tolerance in mice. Brain Res **995:**260–266. http://dx.doi.org/10.1016/j.brainres.2003.09.068.

26. **Chen JK, Lane WS, Schreiber SL.** 1999. The identification of myriocin-binding proteins. Chem Biol **6:**221–235. http://dx.doi.org/10.1016/S1074-5521(99)80038-6.
27. **Humen MA, Perez PF, Lievin-Le Moal V.** 2011. Lipid raft-dependent adhesion of *Giardia intestinalis* trophozoites to a cultured human enterocyte-like Caco-2/TC7 cell monolayer leads to cytoskeleton-dependent functional injuries. Cell Microbiol **13:**1683–1702. http://dx.doi.org/10.1111/j.1462-5822.2011.01647.x.
28. **Mielich-Suss B, Schneider J, Lopez D.** 2013. Overproduction of flotillin influences cell differentiation and shape in *Bacillus subtilis*. mBio **4**(6)**:** e00719-13. http://dx.doi.org/10.1128/mBio.00719-13.
29. **Stuermer CA.** 2011. Microdomain-forming proteins and the role of the reggies/flotillins during axon regeneration in zebrafish. Biochim Biophys Acta **1812:**415–422. http://dx.doi.org/10.1016/j.bbadis.2010.12.004.
30. **Simons K, Ehehalt R.** 2002. Cholesterol, lipid rafts, and disease. J Clin Invest **110:**597–603. http://dx.doi.org/10.1172/JCI16390.
31. **Simons K, Toomre D.** 2000. Lipid rafts and signal transduction. Nat Rev Mol Cell Biol **1:**31–39. http://dx.doi.org/10.1038/35036052.
32. **Silva L, Coutinho A, Fedorov A, Prieto M.** 2006. Competitive binding of cholesterol and ergosterol to the polyene antibiotic nystatin. A fluorescence study. Biophys J **90:**3625–3631. http://dx.doi.org/10.1529/biophysj.105.075408.
33. **Lauwaet T, Davids BJ, Reiner DS, Gillin FD.** 2007. Encystation of *Giardia lamblia*: a model for other parasites. Curr Opin Microbiol **10:**554–559. http://dx.doi.org/10.1016/j.mib.2007.09.011.
34. **Yichoy M, Nakayasu ES, Shpak M, Aguilar C, Aley SB, Almeida IC, Das S.** 2009. Lipidomic analysis reveals that phosphatidylglycerol and phosphatidylethanolamine are newly generated phospholipids in an early-divergent protozoan, *Giardia lamblia*. Mol Biochem Parasitol **165:**67–78. http://dx.doi.org/10.1016/j.molbiopara.2009.01.004.
35. **Lujan HD, Mowatt MR, Byrd LG, Nash TE.** 1996. Cholesterol starvation induces differentiation of the intestinal parasite *Giardia lamblia*. Proc Natl Acad Sci U S A **93:**7628–7633.
36. **Argüello-Garciá R, Bazán-Tejeda ML, Ortega-Pierres G.** 2009. Encystation commitment in Giardia duodenalis: a long and winding road. Parasite **16:**247–258. http://dx.doi.org/10.1051/parasite/2009164247.
37. **Hata K, Koseki K, Yamaguchi K, Moriya S, Suzuki Y, Yingsakmongkon S, Hirai G, Sodeoka M, von Itzstein M, Miyagi T.** 2008. Limited inhibitory effects of oseltamivir and zanamivir on human sialidases. Antimicrob Agents Chemother **52:**3484–3491. http://dx.doi.org/10.1128/AAC.00344-08.
38. **Morimoto K, Nakakariya M, Shirasaka Y, Kakinuma C, Fujita T, Tamai I, Ogihara T.** 2008. Oseltamivir (Tamiflu) efflux transport at the blood-brain barrier via P-glycoprotein. Drug Metab Dispos **36:**6–9. http://dx.doi.org/10.1124/dmd.107.017699.
39. **Rosa IDA, Atella G, Benchimol M.** 2014. Tritrichomonas foetus diplays classical detergent-resistant membrane microdomains on its cell surface. Protist **165:**293–304. http://dx.doi.org/10.1016/j.protis.2014.03.006.
40. **Bemrick WJ.** 1963. A comparison of seven compounds for giardiacidal activity in Mus musculus. J Parasitol **49:**819–823. http://dx.doi.org/10.2307/3275929.